Zinc vacancies in the heteroepitaxy of ZnO on sapphire: Influence of the substrate orientation and layer thickness

A. Zubiaga,[a] F. Tuomisto, F. Plazaola,[a],[b] and K. Saarinen
Laboratory of Physics, Helsinki University of Technology, 02150 Espoo, Finland

J. A. Garcia
Fisika Aplikatua II Saila, Euskal Herriko Unibertsitatea, P.K. 644, 48080 Bilbao, Spain

J. F. Rommeluere
CNRS-LPS, 1 Place A. Briand, F-92195 Meudon, Cedex, France

J. Zuñiga-Pérez and V. Muñoz-Sanjosé
Universitat de València, Departamento de Fisica Aplicada i Electromagnetisme, Dr. Moliner 50, 46100 Burjassot, Valencia, Spain

Positron annihilation spectroscopy has been used to study the vacancy-type defects produced in films grown by metalorganic chemical vapor deposition on different sapphire orientations. Zn vacancies are the defects controlling the positron annihilation spectra at room temperature. Close to the interface (<500 nm) their concentration depends on the surface plane of sapphire over which the ZnO film has been grown. The Zn vacancy content in the film decreases with thickness, and above 1 μm it is independent of the substrate orientation. © *2005 American Institute of Physics*. [DOI: 10.1063/1.1855412]

Due to its relative low cost, its availability in large area wafers, and its transparency up to about 6 μm light wavelength, sapphire is a potential substrate for mass production of ZnO films. However, the heteroepitaxy of ZnO on sapphire presents several problems due to differences in their chemical and physical properties.[1]

Undoped ZnO is usually *n*-type and excess electrons are considered to be introduced by the presence of hydrogen,[2] Zn interstitials (Zn_i) and/or oxygen vacancies (V_O).[3-5] The *n*-type character typically introduces compensating acceptor defects. Among them, vacancy-like defects have low formation energies according to calculations. Furthermore, they can be experimentally detected as positron traps if they are neutral or negatively charged.

There are several reports focused on the study of the positron behavior in ZnO as single crystals and layers,[6-9] in addition to ion-implantation effects on ZnO[10] and the study of implantation-induced defects. Recently, several papers pointed out the differences in ZnO layers grown on different substrates and on different orientations of sapphire substrates (Ref. 11, and references therein).

We have applied positron annihilation spectroscopy to study open volume defects formed in ZnO samples during growth by metalorganic chemical vapor deposition (MOCVD) on differently oriented sapphire substrates. These substrates show different deposition characteristics that make them useful in technical applications and an understanding of the type and concentration of those defects will allow in-depth knowledge of the resulting films.

ZnO films were grown at atmospheric pressure in a horizontal MOCVD reactor (MR Semicon 102) with a two-inlet configuration, avoiding pre-reactions in the gas phase be-

tween the zinc and oxygen precursors: dimethylzinc-triethylamine (DMZn-TEN) and tertiary-butanol (t-butanol). The total nitrogen flow rate through the reaction chamber was kept constant at 5.6 l/min, while the partial pressures of the precursors had a pressure ratio $R_{VI/II}=5$.

Sapphire substrates of different orientations $(1, 1, -2, 0)$ $(0, 0, 0, 1)$ and $(1, 0, -1, 0)$ (referred to as *a*, *c*, and *m* planes, respectively) were used as received. All the layers were
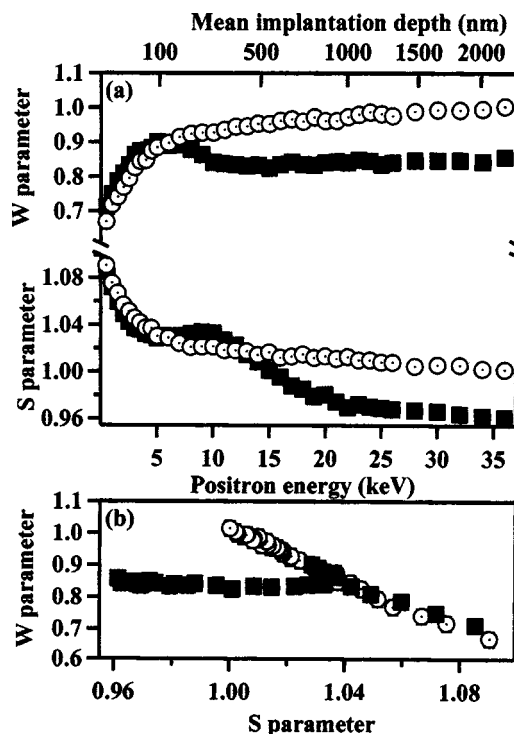

FIG. 1. ZnO reference sample (open circle) and ZnO film grown over *m*-plane sapphire (closed square). (a) *S* and *W* parameters vs energy of the implanted positrons and (b) *W*/*S* plot.

[a] Permanent address: Elektrika&Elektronika eta Fisika Aplikatua II Sailak, Euskal Herriko Unibertsitatea, P.K. 644, 48080 Bilbao, Spain.
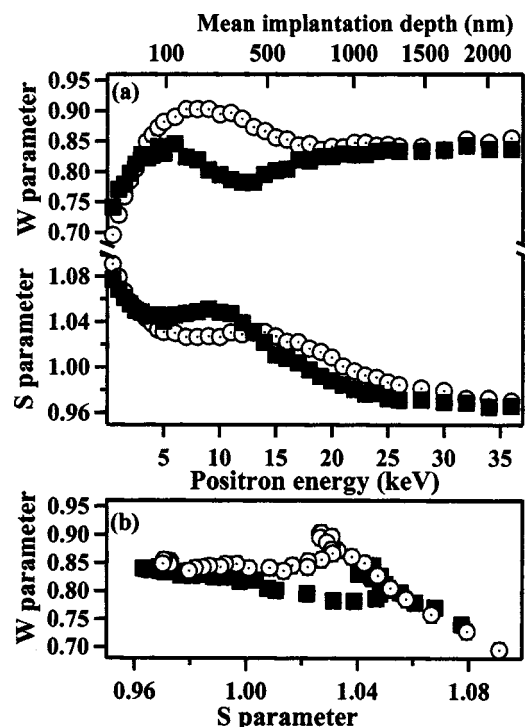[b] Electronic mail: fernando@we.lc.ehu.es

FIG. 2. ZnO films grown over *c*-plane sapphire for 1000 s (closed square) and 7200 s (open circle). (a) *S* and *W* parameters vs energy of the implanted positrons and (b) *W/S* plot.

FIG. 3. *W/S* plot of the cusp positions in all the studied ZnO films.

grown at 420 °C without any prior heat treatment of the substrates. The deposition time was of 1000 s for all the samples resulting in thicknesses around 500 nm. For more details see Ref. 11. An undoped single crystal from Eagle Picher, which did not present traps for positrons at room temperature and has a positron lifetime of 170 ps,[8] was studied as reference.

The experiments were performed at room temperature with a monoenergetic slow positron beam in the 0–40 keV range. The Doppler broadening of the annihilation radiation was measured using a Ge detector with an energy resolution of 1.24 keV at 511 keV. The energy windows, which were used to define the *S* and *W* parameters, were $|E\gamma\text{-}511\text{ keV}| < 0.8$ keV $(p_L/m_0c \leqslant 3\times10^{-3}$, where m_0 is the electron mass) for the central *S* parameter and 2.9 keV $< |E\gamma\text{-}511\text{ keV}| < 7.4$ keV $(11\times10^{-3} \leqslant p_L/m_0c \leqslant 29\times10^{-3})$ for the wing *W* parameter.

Figure 1 shows *W* and *S* parameters versus positron implantation energy and mean implantation depth $(\langle z \rangle = AE^n/\rho$; ρ is the material density and n and A are 1.6 and 4 $\times 10^{-6}$ g cm^{-2} keV$^{-1.6}$, respectively) obtained in the reference sample. The *W/S* plot of the reference sample shows a straight line [open circles in Fig. 1(b)] where the upper left corner corresponds to *W* and *S* parameters of ZnO-bulk. The straight line indicates that there are only two states where positrons annihilate. At very low implantation energies the positrons are preferentially annihilating from surface states (bottom right corner in the figure), but at high implantation energies almost all the positrons are annihilating from delocalized states in the bulk material.

Figure 1 also shows the totally different behavior presented by *S* and *W* parameters in ZnO films grown over *m*-plane sapphire. Both parameters show a small bump for positron implantation energies within the range 5–15 keV, corresponding t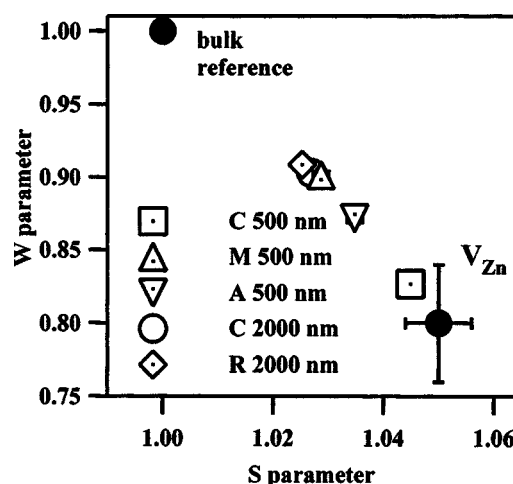o a penetration depth in the order of film thickness. At very low implantation energies positrons are annihilating mainly from surface states [bottom right corner in Fig. 1(b)]. At higher implantation energies the *W/S* plot follows a straight line toward a cusp whose maximum depends on the measured film. The cusp position corresponds to the relative maximum (minimum) of the *W* parameter (*S* parameter) versus implantation energy found in Fig. 1(a). This is a clear indication that in the 0–5 keV range positrons are annihilating from states at the surface and the bulk of the film. Supporting the previous indication, at implantation energies higher than the one corresponding to the cusp the measured values do not follow the previous straight line and they tend toward a new position. The position obtained at the highest implantation energies must correspond to positron annihilation at the bulk of the sapphire. As a consequence of the analysis, and taking into account that the positron mean penetration depth corresponding to the cusp position is about 100 nm, we can conclude that the highest positron annihilation probability at the bulk of ZnO films occur at the cusp of the *W/S* plot.

The $S(E)$ curve at low implantation energies represents positron back-diffusion probability to the surface, from which the positron diffusion length can be estimated by solving the diffusion equation in the conventional way.[12] The obtained value is 50±5 nm in agreement with the values reported in ZnO grown homoepitaxially[6] and over ScAlMgO4 substrates.[7] These values are about five times lower than the lateral grain sizes measured by scanning force microscopy in these samples (above 180 nm in all the cases). However, a small contribution from grain boundaries to the positron annihilation spectra may arise.

To study the influence of the layer thickness on the quality of the grown films, ZnO was grown over *c* plane and $(1,-1,0,2)$ sapphire (*r* plane) for 2 h, under the same conditions as the previous samples. Figure 2 shows the comparison of the *W* and *S* parameters obtained in films grown on *c*-plane sapphire for two different deposition times. The features of the curves corresponding to *W* and *S* parameters of the film grown for 7200 s are wider than the ones of the film grown for 1000 s. The *W/S* plot [Fig. 2(b)] clearly indicates that increasing the thickness of the film grown over *c*-plane sapphire, the cusp of the *W/S* plot moves toward values closer to the bulk value in ZnO.

Figure 3 shows the cusp positions in all the studied ZnO

TABLE I. Zn vacancy concentration (C_{VZn}) in ZnO films grown over different planes of sapphire.

Growth time (s)	Thickness (nm)	Growth plane	C_{VZn} (ppm)
1000	500	*m*	2.0(3)
1000	500	*a*	3.7(8)
1000	500	*c*	7(2)
7200	2000	*c*	1.9(3)
7200	2000	*r*	1.7(3)

films. The W and S parameters of the bulk reference sample and the saturated trapping at Zn vacancies are presented too. The parameters of saturation trapping at Zn vacancies have been estimated from simultaneous lifetime and Doppler measurements in electron irradiated single crystal ZnO.[8] All the measured cusp values fall within a straight line whose slope amounts to $-3.67(5)$. This is a clear indication that the same type of defect, the Zn vacancy, is responsible for the trapping at the ZnO films studied in the present work.

The concentration of Zn vacancies (Table I) has been obtained from the experimental data through the kinetic trapping model.[12] Taking into account the general behavior of the trapping rate[13] and the similarities between ZnO and GaN, we have assumed the positron trapping coefficient of Zn vacancies on the order of 3×10^{15} s^{-1} at 300 K as for the Ga vacancy in that nitride.[14]

The concentration of Zn vacancies depends on the plane of sapphire over which the film has been grown. In films grown for 1000 s the minimum vacancy concentration has been found in the film grown over the *m*-plane orientation where scanning force microscope reveals flat surfaces. However, the *a*, *c* planes of sapphire present well-defined stepped surfaces[11] that produce a different morphology. This different morphology seems to be significant on the Zn vacancy concentration, even for samples 500 nm thick. This could be evidence of a different internal microstructure of grains even at long distances from the interface.

The Zn vacancy concentration of the ZnO film grown over the *c* plane of sapphire decreases about four times when increasing the film thickness from about 500 to 2000 nm. It is interesting to notice that in the case of ZnO grown for 2 h over the *r*-plane sapphire, the concentration of Zn vacancies is very close to the one found in thick ZnO film grown over *c*-plane sapphire. The dependence on film thickness is similar to the one found in the heteroepitaxy of GaN[15] and InN[16] on sapphire. In the nitrides, the thickness dependence of vacancy concentration can be associated with increased doping

due to oxygen diffusion from the substrate, leading to higher concentration of compensating vacancies. However, in ZnO oxygen diffusion from sapphire should not have such a role. Therefore, the presented results indicate that the largest vacancy concentration induced in the film occurs at the first steps of the growth, probably caused by the misorientation of the substrate planes.

In summary, Zn vacancies are the defects giving contribution to the annihilation spectra in ZnO grown by metalorganic chemical vapor deposition on sapphire. Their concentration depends on the surface plane of sapphire over which the ZnO film has been grown. A correlation between the misorientation of the sapphire surface planes and the concentration of vacancies in the films have been observed for thin (<500 nm) films, but this correlation disappears for thicker (>1000 nm) films. Moreover, the defect content in the film depends on the thickness of the film, and it is larger close to the interface.

[1] D. F. Croxall, R. C. C. Ward, C. A. Wallace, and R. C. Kell, J. Cryst. Growth **22**, 117 (1974).

[2] D. H. Hofmann, A. Hofstaetter, F. Leiter, H. Zhou, F. Henecker, B. K. Meyer, S. B. Orlinskii, J. Schmidt, and P. G. Baranov, Phys. Rev. Lett. **88**, 045504-1 (2002).

[3] K. I. Hagemark, J. Solid State Chem. **16**, 293 (1976).

[4] G. D. Mahan, J. Appl. Phys. **54**, 3825 (1983).

[5] A. F. Kohan, G. Ceder, D. Morgan, and Chris. G. Van de Walle, Phys. Rev. B **61**, 15019 (2000).

[6] T. Koida, S. F. Chichibu, A. Uedono, A. Tsukazaki, M. Kawasaki, T. Sota, Y. Segawa, and H. Koinuma, Appl. Phys. Lett. **82**, 532 (2003).

[7] A. Uedono, T. Koida, A. Tsukazaki, M. Kawasaki, Z. Q. Chen, S. F. Chichibu, and H. Koinuma, J. Appl. Phys. **93**, 2481 (2003).

[8] F. Tuomisto, V. Ranki, K. Saarinen, and D. C. Look, Phys. Rev. Lett. **91**, 205502 (2003).

[9] Z. Q. Chen, S. Yamamoto, M. Maekawa, A. Kawasuso, X. L. Yuan, and T. Sekiguchi, J. Appl. Phys. **94**, 4807 (2003).

[10] Z. Q. Chen, M. Maekawa, S. Yamamoto, A. Kawasuso, X. L. Yuan, T. Sekiguchi, R. Suzuki, and T. Ohdaira, Phys. Rev. B **69**, 035210 (2004).

[11] C. Munuera, J. Zúñiga-Pérez, J. F. Rommeluer, V. Sallet, R. Triboulet, F. Soria, V. Muñoz-San José, and C. Ocal, J. Cryst. Growth **264**, 70 (2004).

[12] K. Saarinen, P. Hautojärvi, and C. Corbel, in *Identification of Defects in Semiconductors*, edited by M. Stavola (Academic, New York, 1998).

[13] M. J. Puska, C. Corbel, and R. M. Nieminen, Phys. Rev. B **41**, 9980 (1990).

[14] K. Saarinen, T. Suski, I. Grzegory, and D. C. Look, Phys. Rev. B **64**, 233201 (2001).

[15] J. Oila, J. Kivioja, V. Ranki, K. Saarinen, D. C. Look, R. J. Molnar, S. S. Park, S. K. Lee, and J. Y. Han, Appl. Phys. Lett. **82**, 3433 (2003).

[16] J. Oila, A. Kemppinen, A. Laakso, K. Saarinen, W. Egger, L. Liszkay, P. Sperr, H. Lu, and W. J. Schaff, Appl. Phys. Lett. **84**, 1486 (2004).